Cancer Letters 440–441 (2019) 135–144

Contents lists available at ScienceDirect

Cancer Letters

journal homepage: www.elsevier.com/locate/canlet

Original Articles

2,3,7,8-Tetrachlorodibenzo-p-dioxin (TCDD) induces peripheral blood abnormalities and plasma cell neoplasms resembling multiple myeloma in mice

Lei Wang[a,b,1], Munish Kumar[b,c,1], Qipan Deng[b], Xu Wang[b], Ming Liu[b,d], Zhaojian Gong[b,e], Shanshan Zhang[b,f], Xiaodong Ma[a,b], Zijun Y. Xu-Monette[g], Min Xiao[g], Qing Yi[b], Ken H. Young[g], Kenneth S. Ramos[h], Yong Li[b,*]

[a] Institute for Brain Research and Rehabilitation, South China Normal University, Guangzhou, China
[b] Department of Cancer Biology, Lerner Research Institute, Cleveland Clinic, Cleveland, OH, USA
[c] Raman Fellow (UGC), Department of Biochemistry, University of Allahabad, Allahabad, India
[d] State Key Laboratory of Respiratory Diseases, Guangzhou Institute of Respiratory Diseases, The First Affiliated Hospital of Guangzhou Medical University, Guangzhou Medical University, Guangzhou, China
[e] Department of Stomatology, The Second Xiangya Hospital, Central South University, Changsha, China
[f] Department of Stomatology, Xiangya Hospital, Central South University, Changsha, China
[g] Department of Hematopathology, The University of Texas MD Anderson Cancer Center, Houston, TX, USA
[h] Division of Pulmonary, Allergy, Critical Care and Sleep Medicine, College of Medicine, University of Arizona, Tucson, AZ, USA

ARTICLE INFO

Keywords:
TCDD
Multiple myeloma
Vk*Myc
Mice

ABSTRACT

Although epidemiologic studies have suggested a possible association between occupational exposures to 2,3,7,8-tetrachlorodibenzo-p-dioxin (TCDD) and the risk of development of multiple myeloma, definitive evidence in support of this association is lacking. In the present study, we employed the Vk*Myc mouse model of multiple myeloma to assess the impact of TCDD exposure on multiple myeloma pathogenesis. TCDD induced splenomegaly and multiple peripheral blood abnormalities, including anemia and high serum IgG levels. In addition, TCDD triggered bone lytic lesions, as well as renal tubular casts, a phenomenon associated with human myeloma kidney disease. Even in wild-type C57BL/6 mice, TCDD increased serum IgG levels, induced anemia, and increased plasma cell presence in the spleen and bone marrow, hallmarks of benign monoclonal gammopathy. Lastly, TCDD induced AKT activation and the DNA damage response, key pathogenic events in myeloma pathogenesis, in animal spleen and/or bone marrow. These data indicate that TCDD accelerates monoclonal gammopathy development and promotes progression to multiple myeloma in genetically-predisposed mice. This work offers the first direct experimental evidence establishing TCDD as an environmental risk factor for monoclonal gammopathy of undetermined significance and multiple myeloma.

1. Introduction

Multiple myeloma is a plasma cell neoplasm and the second most common hematological malignancy in the United States. An estimated 30,770 new cases of multiple myeloma and 12,770 deaths caused by multiple myeloma has been predicted in the United States in 2018 [1]. Virtually all multiple myeloma cases are preceded by a precursor condition, monoclonal gammopathy of undetermined significance (MGUS), and the prevalence of MGUS increases with age, ranging from 1.7% among individuals 50–59 years of age to 5% in those older than 70 years [2]. The risk of progression from MGUS to multiple myeloma is estimated to be 1% per year [3,4]. Despite significant medical advances in multiple myeloma drug development in the last 20 year, multiple myeloma is still considered incurable. Multiple myeloma is regarded as a disease with environmental causes, yet its etiology and what prompts progression remain largely unclear.

Dioxins are a group of chemically related compounds that are persistent organic pollutants. Among all dioxin compounds, 2,3,7,8-tetrachlorodibenzo-p-dioxin (TCDD) is a highly toxic environmental contaminant of particular concern for veterans of the Vietnam War who

* Corresponding author.
E-mail address: liy2@ccf.org (Y. Li).
[1] These authors contribute equally to this project.

https://doi.org/10.1016/j.canlet.2018.10.009
Received 7 June 2018; Received in revised form 11 September 2018; Accepted 9 October 2018

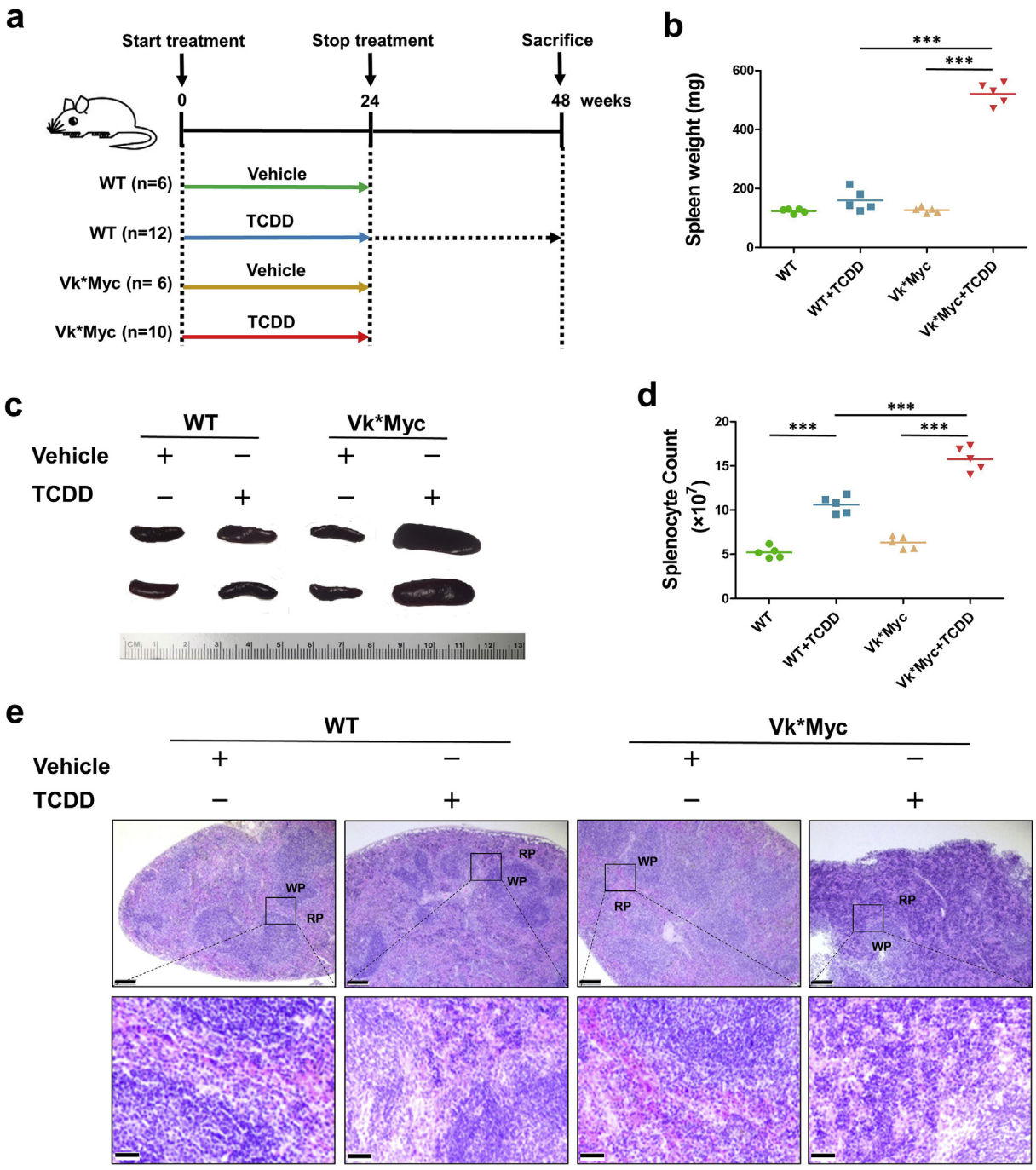

Fig. 1. TCDD treatment promotes splenomegaly in Vk*Myc mice. (a) Schematic diagram of the experimental exposure regimen used in all 4 groups. (b) Mouse spleen weight at 48 weeks. (c) Representative images of spleens from 4 groups of mice (2 from each group). (d) The total number of splenocytes per spleen from mice at sacrifice. (e) Representative H&E-stained spleen sections from TCDD-treated Vk*Myc mice showing altered architecture with a reduction of lymphoid white pulp (WP) and an expansion of hematogenous red pulp (RP). Scale bar = 200 μm (top) or 25 μm (bottom). Data in (b and d) were analyzed by one-way ANOVA. The horizontal lines were presented as the mean value. n = 5 mice per group. *, P ≤ 0.05; **, P ≤ 0.01; ***, P ≤ 0.001. (For interpretation of the references to colour in this figure legend, the reader is referred to the Web version of this article.)

may have been exposed to TCDD during theater use of Agent Orange as an herbicide. While TCDD is not produced commercially, except as a pure compound for scientific and biomedical research, it is formed as a byproduct of herbicide synthesis or in burning processes from waste incineration, metals production, and fossil-fuel and wood combustion. Due to the omnipresence of TCDD, virtually everyone world-wide has some background exposure to this agent. The significance of these environmental exposures remains hotly debated.

TCDD is identified a known human carcinogen by the International Agency for Research on Cancer (IARC) of the World Health Organization [5]. In IARC's most recent review monograph, overall, the strongest evidence for TCDD carcinogenicity is for all cancers combined, rather than for any specific site [5]. In addition, the association of TCDD exposure with lung cancer, sarcoma, and non-Hodgkin lymphoma is stronger than that for other cancers, including multiple myeloma. As noted, TCDD has also been extensively studied for health effects linked to its presence as a contaminant in the herbicide Agent Orange, which was sprayed widely during the Vietnam War [6]. A

committee of the Health and Medicine Division of the National Academies of Sciences, Engineering, and Medicine released the most recent report on exposure of veterans to Agent Orange, which concluded that evidence is sufficient for as association between Agent Orange exposure in Vietnam veterans and sarcoma, Hodgkin lymphoma, and non-Hodgkin lymphoma, but evidence is limited/suggestive for multiple myeloma, prostate cancer, and lung cancer [7]. Studies of exposure during the 2001 World Trade Center disaster have reported an increased risk of multiple myeloma in early responders and recovery workers [8,9], who were most likely exposed to substantial doses of carcinogens, including TCDD [9]. A recent publication reports a 2.4-fold increased risk for MGUS in Vietnam veterans than a cohort of control veterans and high serum TCDD levels associated with high M-protein levels in all veterans [10]. However, these studies are associative in nature and only provide indirect evidence. To the best of our knowledge, no direct experimental evidence exists to support TCDD as an environmental carcinogen for multiple myeloma, as rodents exposed to TCDD develop lung tumors, renal tumors, and non-Hodgkin lymphomas rather than multiple myeloma [11,12]. Further, immunoglobin levels in these exposed animals have never been followed to assess for benign monoclonal gammopathy (the mouse equivalent of human MGUS) [11,12].

The *MYC* oncogene is activated in 67% of cases of multiple myeloma but not in MGUS, suggesting that *MYC* activation may be key in the transition to MM [13,14]. Bergsagel and colleagues generated a conditional transgenic mouse model (Vk*Myc) with sporadic, activation-induced deaminase-dependent Myc activation in germinal center B cells. These mice develop benign monoclonal gammopathy, which progresses to multiple myeloma after 70 weeks [14]. This model is regarded as the best available mouse model of multiple myeloma because it recapitulates many of the biological and clinical features of human disease, including progression from MGUS to MM, target organ damage, anemia, and the “M-spike” (elevated serum IgG) [27]. It should be noted that the Vk*Myc mouse line is generated in a C57bl/6 genetic background and that 2-year-old wild-type (WT) C57bl/6 mice have a high incidence of benign monoclonal gammopathy, which rarely progress to multiple myeloma [15]. Thus, aging WT C57bl/6 and Vk*Myc mice are genetically predisposed to monoclonal gammopathy and multiple myeloma and represent suitable models for studying MGUS and multiple myeloma. Given that no rodent models of multiple myeloma have been used in the past to study the impact of TCDD in myeloma pathogenesis, we hypothesized that exposure to TCDD in the Vk*Myc model would reveal whether TCDD is a *bona fide* promoter of multiple myeloma progression. Our data provide compelling evidence that TCDD accelerates benign monoclonal gammopathy in WT mice and promotes multiple myeloma progression in Vk*Myc mice, providing the first direct experimental animal evidence to support TCDD as an environmental causative factor for multiple myeloma.

2. Materials and methods

2.1. Mice

Vk*Myc mice in the C57Bl/6J genetic background were generated and obtained by Dr. Bergsagel and genotyping was performed using PCR as previously reported [14]. Vk*Myc and wild-type (WT) C57BL/6J mice were crossed to obtain littermates of WT and Vk*Myc mice. Sex-matched WT and Vk*Myc mice (8 weeks old) were assigned to a treatment or control group based on body weight. The dosing regimen employed is presented in Fig. 1a. The treatment group was injected intraperitoneally with 2.5 μg TCDD/kg body weight (Sigma-Aldrich, St. Louis, MO) diluted 1:10 in corn oil once a week per mouse for 24 weeks, for a total calculated accumulated TCDD dose of 60 μg/kg body weight. Equal volumes of corn oil per body weigh were injected into WT and Vk*Myc mice as vehicle control groups. Treated mice were then housed without any further treatment for an additional 24 weeks (Fig. 1a). Every 6 weeks, blood from 5 arbitrarily selected mice from each group was drawn and the IgG levels measured. At the end of the 48 weeks, mice were euthanized by isoflurane overdose followed by cervical dislocation. All animal experimentation was carried out in accordance with NIH guidelines and under protocols approved by the Cleveland Clinic Institutional Animal Care and Use Committee.

2.2. Blood assays

A complete blood count (CBC) was determined using the Advia 120 Hematology System (Siemens Healthineers, Erlangen, Germany). To measure total serum IgG, blood was collected into Eppendorf tubes, allowed to coagulate at room temperature for 5 min, and centrifuged for 10 min at 850 g. Total IgG in serum was then determined by ELISA using the Easy-TiterMouse IgG Assay Kit and Mouse IgG Isotype Control (Thermo Fisher Scientific, Rockford, IL) according to the manufacturer's protocol. For serum protein electrophoresis, sera were diluted 1:2 in normal saline buffer and then analyzed on a QuickGel Chamber apparatus using Precasted QuickGels (Helena Laboratories, Beaumont, TX) according to the manufacturer's instructions.

2.3. Flow cytometric analysis

Spleens and bone marrow were harvested from mice and mashed first through a 70-μm and then a 40-μm nylon strainer (Sigma-Aldrich, St. Louis, MO) into RPMI medium to generate single-cell suspensions, which were then treated with ACK (Ammonium-Chloride-Potassium) lysis buffer (Lonza, Anaheim, CA) to remove red blood cells (RBCs). Cells (10×10^6) were suspended in 0.2 mL PBS and incubated with PE anti-mouse CD138 (syndecan-1) (BioLegend, San Diego, CA) and APC Rat Anti-Mouse CD45R/B220 (clone RA3-6B2) (BD Biosciences, San Diego, CA) on ice in the dark room for 15 min. Cells were then washed twice with PBS and resuspended in 0.5 mL PBS; flow cytometric analysis was performed on a MACSQuant Analyzer 10 (BD Biosciences). A total of 1×10^5 events were collected. FlowJo software (BD Biosciences) was used for data analysis.

2.4. Histology and confocal microscopy

For histological examinations, tissues were fixed in 10% neutral buffered formalin, embedded in paraffin, decalcified in 14% EDTA solution (for bone tissues only) and serially sectioned (5 μm thick). Sections were stained with hematoxylin and eosin (H&E). For immunofluorescence analysis, tissue sections (8 μm thick) were fixed in 4% paraformaldehyde, blocked, reacted with the primary antibodies overnight against CD138 (#142503, BioLegend, San Diego, CA) or Ki67 (#ab16667, Abcam, Cambridge, MA), washed, incubated with secondary fluorescent-conjugated antibodies (goat anti-rabbit IgG H&L - Alexa Fluor 488, #ab150077, Abcam) followed by cover slipping with mounting media containing DAPI nuclear stain. Confocal images were acquired using a Leica TCS-SP5 confocal microscope (Leica Microsystems; Buffalo Grove, IL). All histology analyses were performed using 3 sections from 5 animals in each group.

2.5. Western blot analyses

Splenocytes and bone marrow cells (10×10^6) were lysed with RIPA buffer (Thermo Fisher Scientific, Rockford, IL) containing protease and phosphatase inhibitor cocktails (Thermo Fisher Scientific, Rockford, IL); and protein concentration was measured with a BCA protein assay kit (Thermo Fisher Scientific, Rockford, IL). After mixing with Laemmli sample buffer (Bio-Rad Laboratories, Hercules, CA) containing 10% β-mercaptoethanol, the cell lysates were denatured at 95 °C for 5 min. Equal amounts of proteins were loaded on 10%–15% SDS-polyacrylamide gels (Mini-PROTEAN TGX Precast gels, Bio-Rad, Hercules, California); separated proteins were transferred onto PVDF

membranes. The membrane was blocked using 5% nonfat dry milk in TBS-Tween-20 (0.1%, v/v) for 1 h and incubated with primary antibody at 4 °C overnight. The antibodies were purchased from Cell Signaling Technology (Danvers, MA, USA): caspase-3 (#9662), PARP (#9542), p53 (#2524), p-p53 (#9286), PUMA (#7467), Akt (#2920), *p*-Akt (Ser473) (#4060) and β-actin (#3700). p21 (#6246) antibodies were obtained from Santa Cruz Biotechnology (Santa Cruz, CA, USA). Horseradish peroxidase-conjugated anti-rabbit or anti-mouse IgG was used as the secondary antibody. Immunoreactive protein was visualized with the Pierce Dura Western blotting substrate (Thermo Fisher Scientific, Rockford, IL). X-ray film images were quantified by scanning densitometry using area integration.

2.6. Statistics

Statistical analysis was carried out using GraphPad InStat 3 software (GraphPad Software, Inc., San Diego, CA, USA). The statistical significance between the groups was determined by one-way or two-way analysis of variance (ANOVA) with the appropriate *post hoc* testing using Tukey's Test. Significance was set at $P \leq 0.05$.

3. Results

3.1. TCDD induces splenomegaly in Vk*Myc mice

Vk*Myc mice and their WT littermates were given intraperitoneal injections of 2.5 μg/kg TCDD or corn oil for 24 weeks. Animals were monitored at six-week intervals and maintained for an additional 24-week period before sacrifice (Fig. 1a). Gross pathologic analysis of animals at the 48-week necropsy revealed no major internal organ defects, except for a pronounced increase in spleen weights in Vk*Myc mice treated with TCDD compared to corn oil-treated counterparts or TCDD-treated WT mice (Fig. 1b and c). TCDD significantly increased splenocyte numbers per organ in both WT and Vk*Myc mice, with the highest numbers found in Vk*Myc mice treated with TCDD (Fig. 1d). Histopathologic analysis revealed that the spleens of vehicle-treated WT and Vk*Myc mouse had normal splenic organization, with clearly identifiable regions of red and white pulp (Fig. 1e). These histological characteristics were preserved in spleens from WT mice receiving TCDD, but not in spleens of Vk*Myc mice receiving TCDD. Spleens from Vk*Myc mice challenged with TCDD exhibited marked histological disorganization, along with a reduction of lymphoid white pulp and expansion of hematogenous red pulp (Fig. 1e). These findings indicate that TCDD treatment is associated with splenomegaly and this response appears to involve disruption of growth regulatory control in splenocytes. These actions of TCDD were magnified in mice genetically predisposed by activating mutation in the *Myc* gene.

3.2. TCDD-treated Vk*Myc mice develop multiple peripheral blood abnormalities

Serum IgG levels in Vk*Myc mice treated with TCDD did not increase during the 24-week treatment period. However, sharp increases were detected between weeks 24 and 48 after dosing in both WT and Vk*Myc mice treated with TCDD (Fig. 2a). Compared to corn oil treated WT mice where stable IgG levels were measured at all times, TCDD-treated WT mice showed steady increases in IgG levels. In the case of Vk*Myc mice treated with TCDD, IgG levels reached 17.8 g/L compared to 3.8 g/L in vehicle-treated Vk*Myc mice at week 36. By 48 weeks, serum levels of total IgG in Vk*Myc mice treated TCDD increased to about 19.4 g/L, a net increase that represents a > 5-fold of that (3.2 g/L) of vehicle-treated Vk*Myc mice ($p < 0.01$; Fig. 2b). WT mice treated with TCDD also exhibited increased IgG levels compared to corn oil controls, albeit at considerably reduced levels compared to genetically-susceptible Vk*Myc mice. Serum protein electrophoresis (SPEP) analysis was performed for all mice: significant IgG monoclonal peaks, i.e., M-spike, were evident in Vk*Myc mice treated with TCDD, and to a lesser extent in TCDD-treated WT mice (Fig. 2c). None of the vehicle-treated Vk*Myc mice or WT mice had an M-spike. This is the first direct evidence of blood abnormalities consistent with multiple myeloma in mice treated with TCDD, a response that is magnified in mice genetically predisposed to multiple myeloma.

The complete blood count showed multiple blood abnormalities in mice following TCDD treatment. TCDD decreased hemoglobin concentration in both WT and Vk*Myc mice compared to respective controls, but the decrease was markedly pronounced in Vk*Myc mice (Fig. 2d). The red blood cell (RBC) and white blood cell (WBC) counts were also reduced by TCDD (Fig. 2e and f), with significant increases in RBC mean cell volume (MCV) seen in Vk*Myc, but not WT mice (Fig. 2g). The platelet counts and hematocrit (HCT) were also significantly reduced in TCDD-treated Vk*Myc mice (Fig. 2h and i). Overall, TCDD induced blood dyscracias such as anemia in both WT and Vk*Myc mice, with a stronger impact on Vk*Myc mice.

3.3. Progressive plasma cell neoplasms found in Vk*Myc mice treated with TCDD

High CD138 expression in the absence of B220 expression ($CD138^{hi}$ $B220^{-}$) is recognized as a prominent marker profile of plasma cells [16]. To determine if there was expansion of plasma cells, flow cytometry analyses of splenocytes and bone marrow cells were performed. An increase in the numbers of $CD138^{hi}$ $B220^{-}$ cells was detected in both WT and Vk*Myc mice treated with TCDD (Fig. 3a). TCDD-treated WT and Vk*Myc mice harbored an average 2.1% and 4.7% $CD138^{hi}$ $B220^{-}$ plasma cells in spleens, respectively, a significant increase compared with vehicle-treated counterparts (Fig. 3b). Similarly, the bone marrow of TCDD-treated WT and Vk*Myc mice contained approximately 1.5% and 5.8% $CD138^{hi}$ $B220^{-}$ plasma cells, whereas the bone marrow from the vehicle-treated control groups had less than 1% plasma cells (Fig. 3c).

To determine plasma cell localization and compartmentalization in the spleen and bone marrow, we stained sections of spleen and bone marrow using antibodies against $CD138^{+}$ (plasma cells) and $Ki67^{+}$ (a marker for proliferation). $CD138^{+}$ cells were predominantly located in the spleen and bone marrow of TCDD-treated Vk*Myc mice compared to WT TCDD-treated mice. A moderate increase in $Ki67^{+}$ neoplastic plasma cell nuclei was also detected in the spleen (Fig. 3d), but not in the bone marrow (Fig. 3e). These data support that TCDD treatment increases the presences of proliferative plasma cells in the spleen but not in the bone marrow in Vk*Myc mice.

3.4. Target organ damage in mice treated with TCDD

To investigate the degree of target organ damage, bone, spleen, kidney, liver, and lung were sectioned and stained with hematoxylin and eosin (H&E). The bone structure was damaged in TCDD-treated Vk*Myc mice as evidenced by bone lytic lesions in the femoral shaft (Fig. 4a). These lesions extended to the outside surface of the bone. We also observed minor bone lesions in TCDD-treated WT mice and vehicle-treated Vk*Myc mice, but not in vehicle-treated WT mice (Fig. 4a). H&E staining also confirmed the presence of plasma cells in the bone marrow and spleen in TCDD-treated WT and Vk*Myc mice (Fig. 4b). These plasma cells exhibited characteristic features — royal blue cytoplasm, paranuclear clear zone, eccentric round nucleus, and clumped chromatin. Compared with the 3 other groups, more plasma cell nests were found in the bone marrow and spleen of Vk*Myc mice with TCDD treatment (Fig. 4b and c).

Next, we analyzed the histopathologic changes in the kidney, liver, and lung in all groups of mice. Tubular casts, in the form of cell necrosis, were found in the kidneys of both TCDD-treated groups, but not in the vehicle control groups; TCDD-treated WT kidneys had smaller and fewer casts than Vk*Myc mice (Fig. 4d, **upper panel**). TCDD-

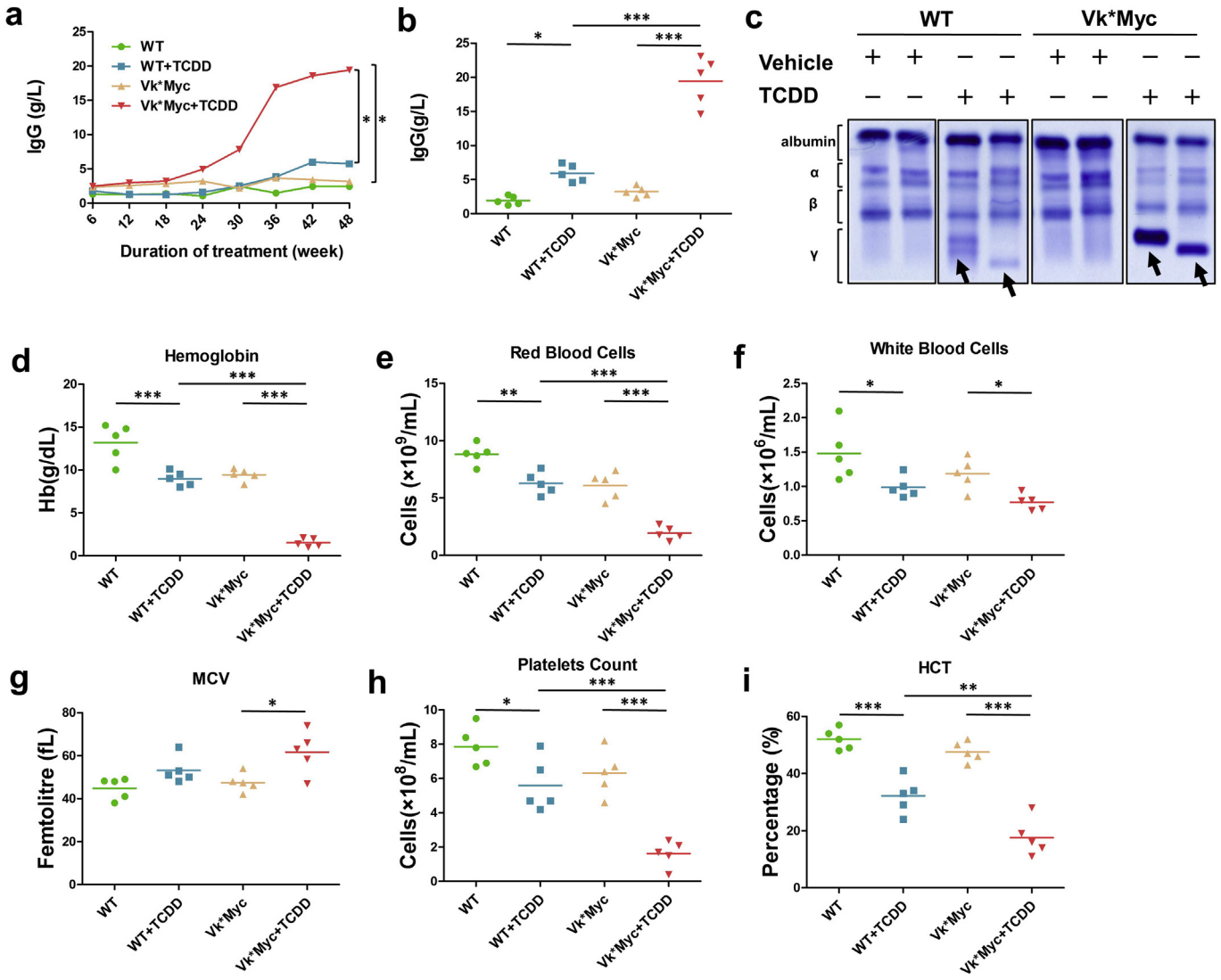

Fig. 2. TCDD-treated Vk*Myc mice develop multiple peripheral blood abnormalities. (a) Total serum IgG levels in mice during 24 weeks of TCDD treatment and the ensuing 24 weeks without treatment. Mice blood samples were collected and assayed for IgG concentration every 6 weeks. (b) Total serum IgG levels in mice at Week 48. (c) Immunoglobins from mice as determined by SPEP at Week 48. Arrows indicate IgG monoclonal peaks (M-spike; γ-globulin peak). SPEP was performed for all mice in each group and representative results of 2 mice per group were shown. (d–i) Complete blood cell counts in mice. Measured blood parameters included (d) hemoglobin (HGB) concentration, (e) red blood cell count (RBC), (f) white blood cell count (WBC), (g) mean red cell volume (MCV), (h) platelets, and (i) hematocrit (HCT). The horizontal lines show the mean values. Data were analyzed by two-way ANOVA (a) or one-way ANOVA (b, d-i). n = 5 mice per group. *, P ≤ 0.05; **, P ≤ 0.01; ***, P ≤ 0.001. (For interpretation of the references to colour in this figure legend, the reader is referred to the Web version of this article.)

treated Vk*Myc mice displayed hepatic fibrosis and collagen deposition, whereas TCDD-treated WT mice showed a less severe phenotypes; the 2 vehicle-treated groups showed normal lobular hepatic architectures (Fig. 4d, **middle panel**). The lungs in TCDD-treated Vk*Myc mice were severely damaged, with destruction of lung alveoli, inflammatory cell infiltration, and thickening of the lung interstitium as compared to the WT counterpart; in contrast, the vehicle-treated WT and Vk*Myc mice showed no significant lung damage (Fig. 4d, **lower panel**). Taken together, these data indicate that TCDD treatment damages multiple organs in both WT and Vk*Myc mice with increased severity of damage in Vk*Myc mice.

3.5. AKT and DNA damage response are activated by TCDD

Because AKT plays a crucial role in intracellular signal transduction pathways that regulate cell growth, survival, transformation, and tumorigenesis [17,18], we determined the status of AKT in mice with TCDD treatment. The activation of AKT in splenocytes was significantly increased in both TCDD-treated WT and Vk*Myc mice; and the response was most pronounced in Vk*Myc mice (Fig. 5a). Likewise, AKT phosphorylation was strong in bone marrow cells from TCDD-treated WT and Vk*Myc mice (Fig. 5b). These findings demonstrate that TCDD treatment induces activation of AKT in the bone marrow and spleen, particularly in Vk*Myc mice.

We determined splenocyte expression of caspase-3 and poly (ADP-ribose) polymerase (PARP). As a marker of apoptosis, cleaved caspase-3 was detected at low levels in mice without TCDD treatment. With TCDD treatment, cleaved caspase-3 was significantly increased in the spleen of both WT and Vk*Myc mice, with Vk*Myc mice having more cleaved caspase-3 than WT mice. Caspase-mediated PARP cleavage was enhanced by TCDD treatment in the spleen of both WT and Vk*Myc mice. We also assessed activation of the p53 signaling pathway (Fig. 5b). The phosphorylation of p53 was induced in both the spleen and bone marrow of Vk*Myc mice by TCDD treatment. In the spleen of TCDD-treated mice, we also detected significant upregulation of two p53 targets, PUMA (p53-upregulated modulator of apoptosis) and p21 (a

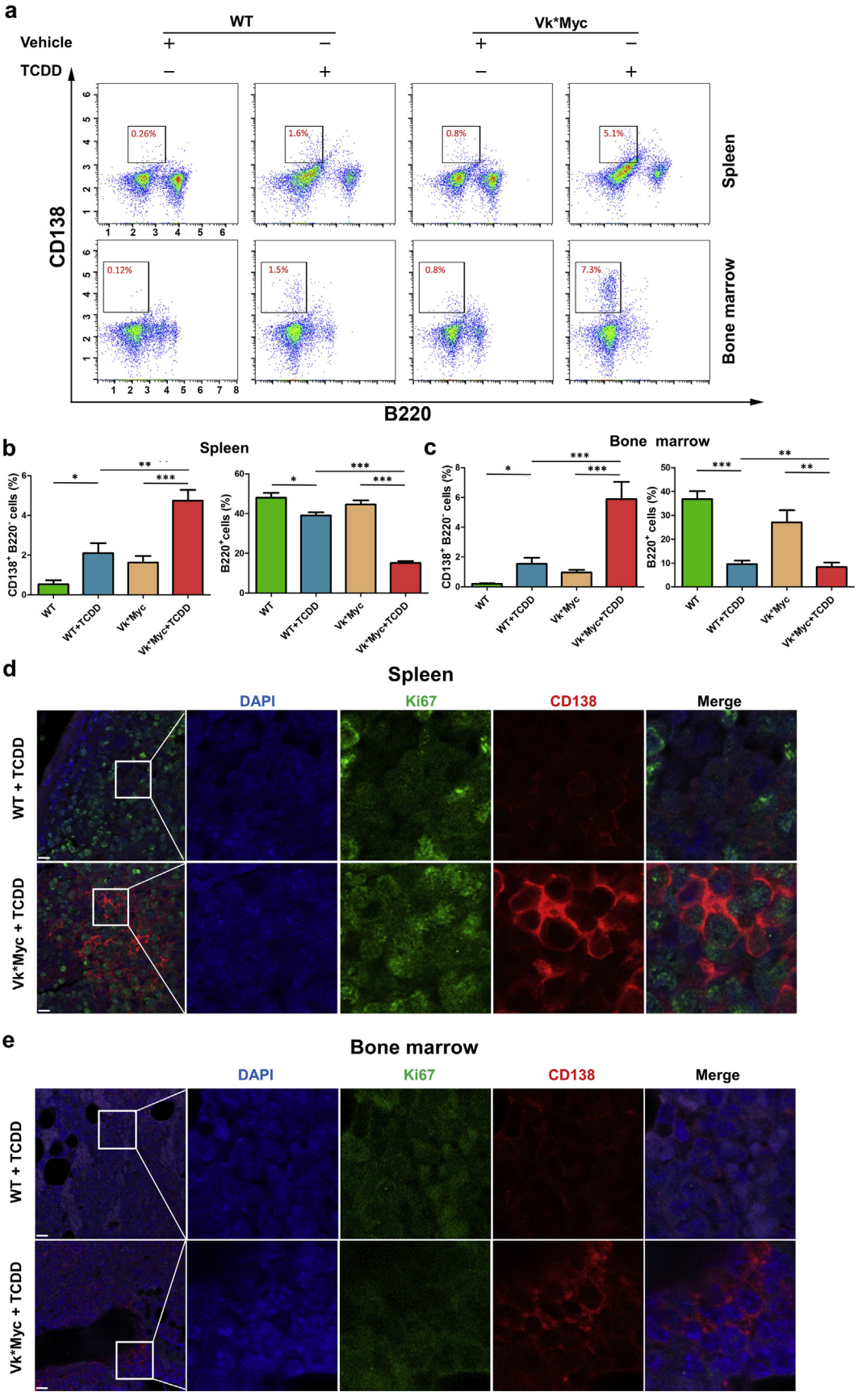

(caption on next page)

Fig. 3. Progressive plasma cell neoplasms in Vk*Myc mice treated with TCDD. (a) Representative flow cytometry plots detecting cell surface markers CD138 (Y-axis) and B220 (X-axis) in splenocytes (upper panel) and bone marrow cells (lower panel). The numbers on the axes denote the $\log_{10}$ values of fluorescence (those of 3 on the right are the same as the ones on the left). The number in the inserts shows the percentage of $CD138^{high}B220^{-}$ cells in the entire cell population. (b, c) Bar graphs of the percentages of $CD138^{+}B220^{-}$ and $B220^{+}$ cells from spleen (b) and bone marrow (c). Data were analyzed by one-way ANOVA. *, $P \leq 0.05$; **, $P \leq 0.01$; ***, $P \leq 0.001$. (d) Confocal microscopy images identifying $Ki67^{+}$ (green) and $CD138^{+}$ (red) expression with nuclear DAPI staining of cells in the spleen of WT (upper panel) and Vk*Myc mice (lower panel) treated with TCDD. Scale bar = 10 μm. (e) Confocal microscopy images identifying $Ki67^{+}$ (green) and $CD138^{+}$ (red) expression with nuclear DAPI staining of cells in the bone marrow of WT (upper panel) and Vk*Myc mice (lower panel) treated with TCDD. Scale bar = 10 μm n = 5 mice per group. (For interpretation of the references to colour in this figure legend, the reader is referred to the Web version of this article.)

cell cycle regulator). We were unable to detect the expression of caspase 3, PARP, Puma, and p21 in the bone marrow in any group. These results demonstrate that TCDD activates Akt and the DNA damage response, particularly in Vk*Myc mice.

4. Discussion

Multiple myeloma is an incurable hematological neoplasm that causes over 10,000 deaths annually in the United States [1]. Multiple myeloma is regarded as an environmental disease, yet its etiology remains largely unclear. The association of multiple myeloma with smoking has been investigated, with some studies suggesting a strong association [19,20], while others refuting this relationship [21–23]. An expert panel reviewing ~40 epidemiologic studies on TCDD, a contaminant hydrocarbon present in Agent Orange, and the risks of multiple myeloma found that there is an elevated risk of multiple myeloma in three fourths of all studies examined [24], but concluded that due to lack of experimental animal data, evidence is limited to support the association of multiple myeloma risk and TCDD exposure. The IARC classified TCDD as a Group 1 human carcinogen in 1997, but its carcinogenic implications in multiple myeloma were poorly understood, and multiple myeloma was only sporadically reported among workers exposed to TCDD [25]. Here, compelling evidence is presented establishing the Vk*Myc mouse line as a valid model to study the impact of TCDD exposure in multiple myeloma pathogenesis.

Multiple myeloma is a clonal B-cell disease of plasma cells that slowly proliferate and secrete IgG proteins. These neoplastic plasma cells grow in the bone marrow, causing bone lesions [26]. Approximately 90% of patients with multiple myeloma develop bone disease, and 80% suffer from bone fractures [27–29]. Even patients with MGUS are at risk for increased bone porosity and reduced bone strength [30,31]. Anemia is also a cardinal feature of multiple myeloma, present in most patients at diagnosis and during follow-up. In our work, following TCDD treatment, Vk*Myc mice have bone lytic lesions and high IgG levels similar to those encountered in patients with multiple myeloma. In addition, TCDD-treated mice demonstrate marked anemia with a decreased hemoglobin concentration and RBC numbers. Splenomegaly is characterized by a marked increase in organ cellularity, which usually rises from compromised extramedullary hematopoiesis, including anemia. Spleen size and weight were strikingly increased in TCDD-treated Vk*Myc mice, suggesting an immune proliferative disorder. CD138 is a transmembrane heparin sulfate proteoglycan normally expressed on plasma cells but not on B-cells. B220 (also known as CD45), a transmembrane protein tyrosine phosphatase, is commonly used as a B cell marker in mice and predominantly expressed on B lymphocytes, including pro-, mature, and activated B cells. Upon TCDD treatment, Vk*MYC mice accumulated terminally differentiated $CD138^{+}B220^{-}$ plasma cells in both the bone marrow and the spleen. Ki-67, as a proliferation-associated nuclear protein, is used to evaluate the proliferative activity of cancer [32,33]. In the bone marrow, proliferating plasma cells is a feature of plasmacytoma, whereas quiescent plasma cells predominate in multiple myeloma [14]. Following TCDD treatment, plenty of cells in the spleen, and a minority of cells in the bone marrow of Vk*Myc mice, co-stained with CD138 and Ki67. TCDD-treated WT mice also exhibited elevated serum IgG levels, reduced hemoglobin and RBC numbers, and increased plasma cells in the bone marrow and spleen, but these changes were mild compared to those in TCDD-treated Vk*Myc mice. Our results indicate that TCDD accelerates MGUS and promotes progression to multiple myeloma in genetically predisposed mice. Given that TCDD is not a mutagen, the degree to which this agent acts to drive oncogenic events and interacts with other environmental triggers of genetic damage to induce MGUS and multiple myeloma in mice or humans remains to be defined.

Renal impairment is an important clinical hallmark of multiple myeloma, being present in up to 50% of patients newly diagnosed with multiple myeloma [34–37]. WT mice treated with TCDD exhibit tubular casts in the kidney, and these casts are larger in TCDD-treated Vk*Myc mice. Previous reports demonstrate that mice with TCDD treatment develop hepatic fibrosis [38–41] and inflammatory pulmonary lesions [42,43], which we also observed in both WT and Vk*Myc mice exposed to TCDD. Several studies have reported lung involvement in human multiple myeloma, including fibrosis, mass lesions, multiple nodular lesions and interstitial infiltrates [44–47]. TCDD is regarded as one of the most potent hepatic carcinogens in rodent models [48]. The observed liver and lung pathology in TCDD-treated mice is likely a direct response to TCDD, rather than a secondary complication of high serum IgG levels. However, renal cast has not been reported in TCDD-treated rodents previously [11]. Thus, tubular casts in the kidney of TCDD-treated Vk*Myc mice is likely a result of the high serum IgG levels, i.e., a complication caused by multiple myeloma progression.

Genes in the RAS signaling pathway, like KRAS and NRAS, are frequently mutated in multiple myeloma [49], and AKT is a major effector pathway of RAS activation. Constitutive activation of AKT is reported to be an oncogenic signal in multiple myeloma and is associated with poor patient prognosis [50]. In this study, we showed that AKT is activated in splenocytes and bone marrow cells in both WT and Vk*Myc mice exposed to TCDD. Cleavage of PARP is a marker for DNA damage and apoptosis [51,52]. We observed that cleaved caspase-3 and cleaved PARP were upregulated in mice with TCDD exposure. As a transcriptional regulator, p53 is activated (phosphorylated) in response to DNA damage, oncogene activation and other stresses, resulting transactivation of p21 and Puma [53,54]. Constitutive ongoing DNA damage is found in human multiple myeloma [55]. In our work, the levels of p53 phosphorylation and p21 and Puma expression in splenocytes and p53 in bone marrow cells were significantly higher in the TCDD-treated mice than in the vehicle-treated control groups, providing evidence suggesting that TCDD exposure induces the DNA damage response. We observed AKT activation and an enhanced DNA damage response at 24 weeks after the completion of TCDD treatment, suggesting the effect of TCDD is indirect or of epigenetic nature.

To summarize, our data provide *in vivo* evidence to support that TCDD accelerates MGUS and promotes disease progression to multiple myeloma and uncover the relevant molecular mechanisms of progression. Previously, definitive evidence is limited to support the association of Agent Orange (i.e., TCDD) exposure in Vietnam veterans and multiple myeloma [7]. Our data, in combination with the epidemiologic study connecting high serum TCDD levels to increased MGUS incidence [10], provides experimental evidence to support that TCDD is an underlying cause for increased prevalence of multiple myeloma and MGUS. Identifying TCDD as a contributing etiologic factor in multiple myeloma and its precursor MGUS opens new doors for cancer prevention for the more than 1 million MGUS patients at risk for the incurable

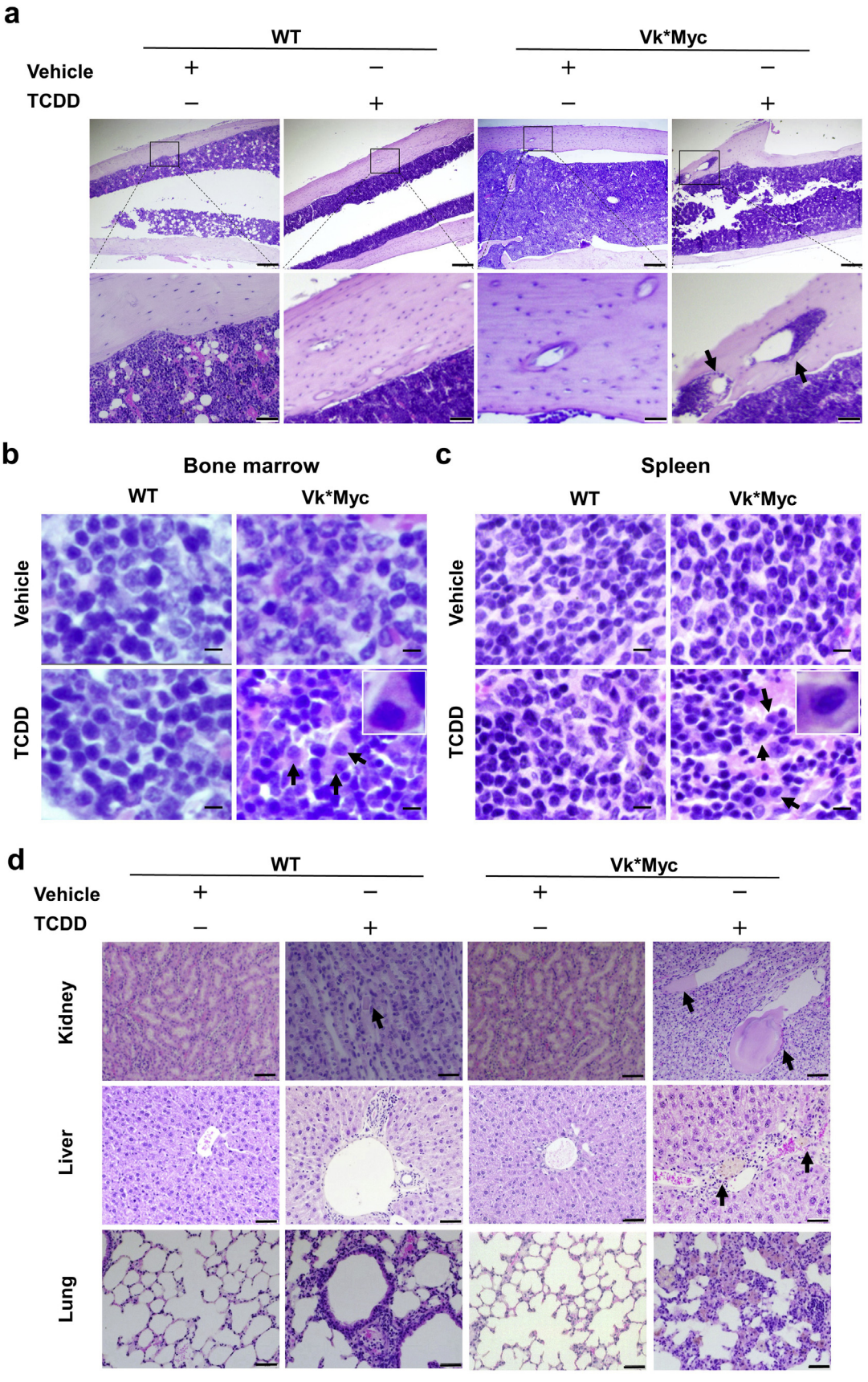

(caption on next page)

Fig. 4. Target organ damage in TCDD-treated mice. (a) Histological evaluation of bone morphology in 4 groups of mice. Bone lytic lesions (indicated by arrows) were detected in the femoral shaft of Vk*MYC mice treated with TCDD. Scale bar = 200 μm (top) or 50 μm (bottom). (b) Infiltrating plasma cells in the bone marrow of TCDD-treated mice. Scale bar = 10 μm. Arrows point to plasma cells. (c) Infiltrating plasma cells in the spleen of TCDD-treated mice. Scale bar = 10 μm. Arrows point to plasma cells. (d) Damage to kidney, liver, and lung. Arrows point to tubular casts in kidney (upper panel, scale bar = 100 μm), collagen deposition in liver (middle panel, scale bar = 50 μm), and destruction of lung morphology (lower panel, scale bar = 50 μm) were observed in TCDD-treated Vk*Myc mice. n = 5 mice per group.

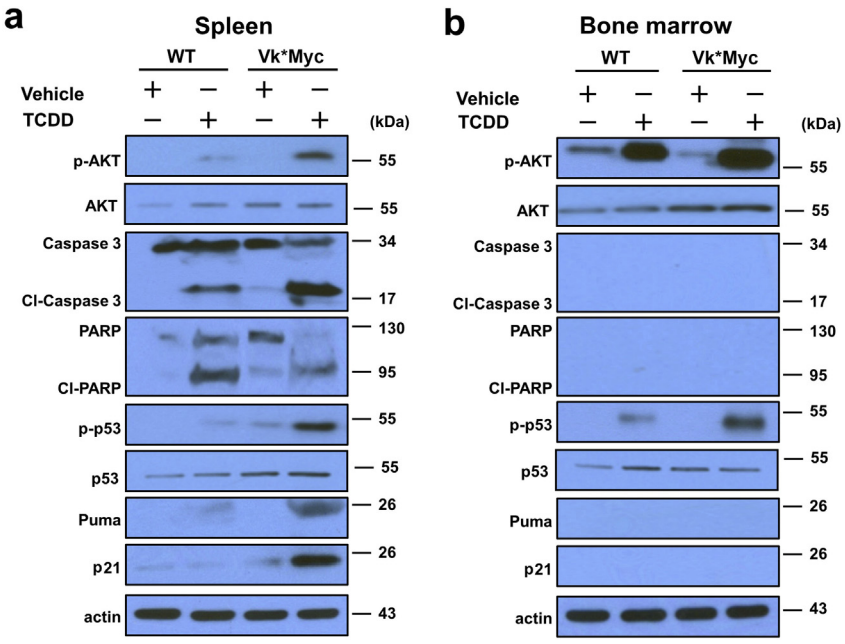

Fig. 5. Splenocytes and bone marrow cells from TCDD-treated mice display AKT activation and markers of the DNA damage response. (a) Western blot analyses of splenocytes from 4 groups of mice. (b) Western blot analyses of bone marrow cells from 4 groups of mice. β-actin was used as a control. n = 5 mice for each group with representative images from 1 animal in each group shown.

multiple myeloma. Because of government regulations, voluntary changes in industrial practices, and improvements in manufacturing, industrial processes are no longer major sources of TCDD in the United States. Yet TCDD has a long enduring half-life in the environment and it is still emitted in uncontrolled waste incinerators and other sources due to incomplete burning. The present study further underscores the relationship between multiple myeloma and TCDD exposure, particularly for those who have MGUS.

Conflicts of interest

The authors declare that they have no financial or non-financial competing interest.

Acknowledgements

LW, MK, KSR, and YL designed the research. All authors performed experiments and/or contributed to data analyses. LW, KSR, and YL wrote the manuscript, and all authors provided critical review and revisions and approved the final version of the manuscript. The authors are grateful to Dr. Cassandra Talerico for editing the manuscript and providing critical comments. This study was supported by NIH R01 grants (CA138688 and CA177810 to YL), National Natural Science Foundation of China (NO. 31500326 to LW), and Natural Science Foundation of Guangdong Province of China (NO. 2017A030313194 to LW).

References

[1] R.L. Siegel, K.D. Miller, A. Jemal, Cancer statistics, 2018, CA A Cancer J. Clin. 68 (2018) 7–30.
[2] R.A. Kyle, T.M. Therneau, S.V. Rajkumar, D.R. Larson, M.F. Plevak, J.R. Offord, A. Dispenzieri, J.A. Katzmann, L.J. Melton, Prevalence of monoclonal gammopathy of undetermined significance, N. Engl. J. Med. 354 (2006) 1362–1369.
[3] I. Turesson, S.A. Kovalchik, R.M. Pfeiffer, S.Y. Kristinsson, L.R. Goldin, M.T. Drayson, O. Landgren, Monoclonal gammopathy of undetermined significance and risk of lymphoid and myeloid malignancies: 728 cases followed up to 30 years in Sweden, Blood 123 (2014) 338–345.
[4] R.A. Kyle, T.M. Therneau, S.V. Rajkumar, J.R. Offord, D.R. Larson, M.F. Plevak, L. Melton, A long-term study of prognosis in monoclonal gammopathy of undetermined significance, N. Engl. J. Med. 346 (2002) 564–569.
[5] R. Baan, Y. Grosse, K. Straif, B. Secretan, F. El Ghissassi, V. Bouvard, L. Benbrahim-Tallaa, N. Guha, C. Freeman, L. Galichet, V. Cogliano, W.I.A.R.C.M. Wo, Special Report: policy A review of human carcinogens-Part F: chemical agents and related occupations, Lancet Oncol. 10 (2009) 1143–1144.
[6] M. Pavuk, J.E. Michalek, A. Schecter, N.S. Ketchum, F.Z. Akhtar, K.A. Fox, Did TCDD exposure or service in southeast Asia increase the risk of cancer in air force Vietnam veterans who did not spray agent orange? J. Occup. Environ. Med. 47 (2005) 335–342.
[7] J. Acquavella, D. Garabrant, G. Marsh, T. Sorahan, D.L. Weed, Glyphosate epidemiology expert panel review: a weight of evidence systematic review of the relationship between glyphosate exposure and non-Hodgkin's lymphoma or multiple myeloma, Crit. Rev. Toxicol. 46 (2016) 28–43.
[8] J.M. Moline, R. Herbert, L. Crowley, K. Troy, E. Hodgman, G. Shukla, I. Udasin, B. Luft, S. Wallenstein, P. Landrigan, D.A. Savitz, Multiple myeloma in world trade center responders: a case series, JOEM (J. Occup. Environ. Med.) 51 (2009) 896–902 810.1097/JOM.1090b1013e3181ad1049c1098.
[9] J. Li, J.E. Cone, A.R. Kahn, et al., ASsociation between world trade center exposure and excess cancer risk, Jama 308 (2012) 2479–2488.
[10] O. Landgren, Y.K. Shim, J. Michalek, et al., Agent orange exposure and monoclonal gammopathy of undetermined significance: an operation ranch hand veteran cohort study, JAMA Oncol. 1 (2015) 1061–1068.
[11] The WHO International Agency for Research on Cancer Monograph Working Group, 2,3,7,8-TCDD, 2,3,4,7,8-PeCDF, and PCB 126, IARC Monographs on the Evaluation of Carcinogenic Risks to Humans, The WHO Press, 2012, pp. 339–378.
[12] R. Baan, Y. Grosse, K. Straif, B. Secretan, F. El Ghissassi, V. Bouvard, L. Benbrahim-Tallaa, N. Guha, C. Freeman, L. Galichet, V. Cogliano, A review of human carcinogens–Part F: chemical agents and related occupations, Lancet Oncol. 10 (2009) 1143–1144.
[13] W.J. Chng, G.F. Huang, T.H. Chung, S.B. Ng, N. Gonzalez-Paz, T. Troska-Price, G. Mulligan, M. Chesi, P.L. Bergsagel, R. Fonseca, Clinical and biological implications of MYC activation: a common difference between MGUS and newly diagnosed multiple myeloma, Leukemia 25 (2011) 1026–1035.
[14] M. Chesi, D.F. Robbiani, M. Sebag, W.J. Chng, M. Affer, R. Tiedemann, R. Valdez, S.E. Palmer, S.S. Haas, A.K. Stewart, R. Fonseca, R. Kremer, G. Cattoretti, P.L. Bergsagel, AID-dependent activation of a MYC transgene induces multiple myeloma in a conditional mouse model of post-germinal center malignancies, Cancer Cell 13 (2008) 167–180.
[15] T.W. van den Akker, E. de Glopper-van der Veer, J. Radl, R. Benner, The influence

of genetic factors associated with the immunoglobulin heavy chain locus on the development of benign monoclonal gammapathy in ageing IgH-congenic mice, Immunology 65 (1988) 31–35.
[16] R.D. Sanderson, M. Borset, Syndecan-1 in B lymphoid malignancies, Ann. Hematol. 81 (2002) 125–135.
[17] B.D. Manning, A. Toker, AKT/PKB signaling: navigating the network, Cell 169 (2017) 381–405.
[18] R. Sever, J.S. Brugge, Signal transduction in cancer, Csh Perspect. Med. 5 (2015).
[19] R.R. Williams, J.W. Horm, Association of cancer sites with tobacco and alcohol consumption and socioeconomic status of patients: interview study from the Third National Cancer Survey, J. Natl. Canc. Inst. 58 (1977) 525–547.
[20] P.K. Mills, G.R. Newell, W.L. Beeson, G.E. Fraser, R.L. Phillips, History of cigarette smoking and risk of leukemia and myeloma: results from the adventist health study, J. Natl. Canc. Inst. 82 (1990) 1832–1836.
[21] P. Fernberg, A. Odenbro, R. Bellocco, P. Boffetta, Y. Pawitan, K. Zendehdel, J. Adami, Tobacco use, body mass index, and the risk of leukemia and multiple myeloma: a nationwide cohort study in Sweden, Cancer Res. 67 (2007) 5983–5986.
[22] T. Psaltopoulou, T.N. Sergentanis, N. Kanellias, P. Kanavidis, E. Terpos, M.A. Dimopoulos, Tobacco smoking and risk of multiple myeloma: a meta-analysis of 40 observational studies, Int. J. Canc. (2012) n/a-n/a.
[23] J.J. Castillo, P.K. Dhami, S. Curry, K. Brennan, No association between cigarette smoking and incidence of plasma cell myeloma: a meta-analysis of 17 observational studies, Am. J. Hematol. 87 (2012) 729–731.
[24] C.t.R.t.H.E.i.V.V.o.E.t, Herbicides, Veterans and Agent Orange: Update 1998, National Academy Press, Washington, D.C., 1999.
[25] R. Baan, Y. Grosse, K. Straif, B. Secretan, F. El Ghissassi, V. Bouvard, L. Benbrahim-Tallaa, N. Guha, C. Freeman, L. Galichet, V. Cogliano, A review of human carcinogens—Part F: chemical agents and related occupations, Lancet Oncol., 10 1143-1144.
[26] M.L. Slovak, Multiple myeloma: current perspectives, Clin. Lab. Med. 31 (2011) 699-+.
[27] L.J. Melton, R.A. Kyle, S.J. Achenbach, A.L. Oberg, S.V. Rajkumar, Fracture risk with multiple myeloma: a population-based study, J. Bone Miner. Res. 20 (2005) 487–493.
[28] C.A. Pappa, G. Tsirakis, F.E. Psarakis, A. Kolovou, M. Tsigaridaki, D. Stafylaki, K. Sfiridaki, M.G. Alexandrakis, Lack of correlation between angiogenic cytokines and serum insulin-like growth factor-1 in patients with multiple myeloma, Med. Oncol. 30 (2013).
[29] S.Y. Kristinsson, A.R. Minter, N. Korde, E. Tan, O. Landgren, Bone disease in multiple myeloma and precursor disease: novel diagnostic approaches and implications on clinical management, Expert Rev. Mol. Diagn 11 (2011) 593–603.
[30] J.N. Farr, W. Zhang, S.K. Kumar, R.M. Jacques, A.C. Ng, L.K. McCready, S.V. Rajkumar, M.T. Drake, Altered cortical microarchitecture in patients with monoclonal gammopathy of undetermined significance, Blood 123 (2014) 647–649.
[31] A.C. Ng, S. Khosla, N. Charatcharoenwitthaya, S.K. Kumar, S.J. Achenbach, M.F. Holets, L.K. McCready, L.J. Melton, R.A. Kyle, S.V. Rajkumar, M.T. Drake, Bone microstructural changes revealed by high-resolution peripheral quantitative computed tomography imaging and elevated DKK1 and MIP-1 alpha levels in patients with MGUS, Blood 118 (2011) 6529–6534.
[32] P. Dziegiel, W. Salwa-Zurawska, J. Zurawski, A. Wojnar, M. Zabel, Prognostic significance of augmented metallothionein (MT) expression correlated with Ki-67 antigen expression in selected soft tissue sarcomas, Histol. Histopathol. 20 (2005) 83–89.
[33] A. Urruticoechea, I.E. Smith, M. Dowsett, Proliferation marker Ki-67 in early breast cancer, J. Clin. Oncol. 23 (2005) 7212–7220.
[34] R. Alexanian, B. Barlogie, D. Dixon, Renal-Failure in multiple-myeloma - pathogenesis and prognostic implications, Arch. Intern. Med. 150 (1990) 1693–1695.
[35] M.A. Dimopoulos, E. Kastritis, L. Rosinol, J. Blade, H. Ludwig, Pathogenesis and treatment of renal failure in multiple myeloma, Leukemia 22 (2008) 1485–1493.
[36] T. Soleymanian, A. Soleimani, A. Musavi, K. Mojtahedi, G. Hamid, Outcome of patients with multiple myeloma and renal failure on novel regimens, Saudi J. Kidney Dis. T 27 (2016) 335–340.
[37] V. Eleutherakis-Papaiakovou, A. Bamias, D. Gika, A. Simeonidis, A. Pouli, A. Anagnostopoulos, E. Michali, T. Economopoulos, K. Zervas, M.A. Dimopoulos, Renal failure in multiple myeloma: incidence, correlations, and prognostic significance, Leuk. Lymphoma 48 (2007) 337–341.
[38] M. Han, X. Liu, S. Liu, G. Su, X. Fan, J. Chen, Q. Yuan, G. Xu, 2,3,7,8-Tetrachlorodibenzo-p-dioxin (TCDD) induces hepatic stellate cell (HSC) activation and liver fibrosis in C57BL6 mouse via activating Akt and NF-kappaB signaling pathways, Toxicol. Lett. 273 (2017) 10–19.
[39] S. Pierre, A. Chevallier, F. Teixeira-Clerc, A. Ambolet-Camoit, L.-C. Bui, A.-S. Bats, J.-C. Fournet, P. Fernandez-Salguero, M. Aggerbeck, S. Lotersztajn, R. Barouki, X. Coumoul, Aryl hydrocarbon receptor–dependent Induction of liver fibrosis by dioxin, Toxicol. Sci. 137 (2014) 114–124.
[40] A.K. Kopec, D.R. Boverhof, R. Nault, J.R. Harkema, C. Tashiro, D. Potter, B. Sharratt, B. Chittim, T.R. Zacharewski, Toxicogenomic evaluation of long-term hepatic effects of TCDD in Immature, ovariectomized C57BL/6 mice, Toxicol. Sci. 135 (2013) 465–475.
[41] R. Nault, K.A. Fader, D.A. Ammendolia, P. Dornbos, D. Potter, B. Sharratt, K. Kumagai, J.R. Harkema, S.Y. Lunt, J. Matthews, T. Zacharewski, Dose-dependent metabolic reprogramming and differential gene expression in TCDD-elicited hepatic fibrosis, Toxicol. Sci. 154 (2016) 253–266.
[42] N. Ishimaru, A. Takagi, M. Kohashi, A. Yamada, R. Arakaki, J. Kanno, Y. Hayashi, Neonatal exposure to low-dose 2,3,7,8-Tetrachlorodibenzo- < em > p < /em > -Dioxin causes autoimmunity due to the disruption of T cell tolerance, J. Immunol. 182 (2009) 6576–6586.
[43] P.S. Wong, C.F. Vogel, K. Kokosinski, F. Matsumura, Arylhydrocarbon receptor activation in NCI-H441 cells and C57BL/6 mice possible mechanisms for lung dysfunction, Am. J. Respir. Cell Mol. 42 (2010) 210–217.
[44] R. Kamble, T. Rosenzweig, Diffuse pulmonary parenchymal involvement in multiple myeloma: antemortem diagnosis, Int. J. Hematol. 83 (2006) 259–261.
[45] Y. Yuan, R. Wieczorek, D.L. Green, P. Cook, H. Ballard, D.J. Araten, Multiple myeloma involving skin and pulmonary parenchyma after autologous stem cell transplantation, J. Hematol. Oncol. 2 (2009).
[46] T. Yokote, T. Akioka, H. Miyamoto, S. Oka, S. Hara, T. Yamano, T. Takasu, M. Tsuji, T. Hanafusa, Pulmonary parenchymal infiltrates in a patient with CD20-positive multiple myeloma, Eur. J. Haematol. 74 (2005) 61–65.
[47] C.S. Chim, M. Wong, Y.S. Fan, Pulmonary interstitial amyloidosis complicating multiple myeloma, J. Clin. Oncol. 26 (2008) 504–506.
[48] S. Knerr, D. Schrenk, Carcinogenicity of 2,3,7,8-tetrachlorodibenzo-p-dioxin in experimental models, Mol. Nutr. Food Res. 50 (2006) 897–907.
[49] J.G. Lohr, P. Stojanov, S.L. Carter, P. Cruz-Gordillo, M.S. Lawrence, D. Auclair, C. Sougnez, B. Knoechel, J. Gould, G. Saksena, K. Cibulskis, A. McKenna, M.A. Chapman, R. Straussman, J. Levy, L.M. Perkins, J.J. Keats, S.E. Schumacher, M. Rosenberg, G. Getz, T.R. Golub, Widespread genetic heterogeneity in multiple myeloma: implications for targeted therapy, Cancer Cell 25 (2014) 91–101.
[50] Y.P. Tu, A. Gardner, A. Lichtenstein, The phosphatidylinositol 3-kinase/AKT kinase pathway in multiple myeloma plasma cells: roles in cytokine-dependent survival and proliferative responses, Cancer Res. 60 (2000) 6763–6770.
[51] M.L. Wang, W.Z. Wu, W.Q. Wu, B. Rosidi, L.H. Zhang, H.C. Wang, G. Iliakis, PARP-1 and Ku compete for repair of DNA double strand breaks by distinct NHEJ pathways, Nucleic Acids Res. 34 (2006) 6170–6182.
[52] M. Aguennouz, G.L. Vita, S. Messina, A. Cama, N. Lanzano, A. Ciranni, C. Rodolico, R.M. Di Giorgio, G. Vita, Telomere shortening is associated to TRF1 and PARP1 overexpression in Duchenne muscular dystrophy, Neurobiol. Aging 32 (2011) 2190–2197.
[53] J.D. Robertson, S. Orrenius, Molecular mechanisms of apoptosis induced by cytotoxic chemicals, Crit. Rev. Toxicol. 30 (2000) 609–627.
[54] D.R. Green, G. Kroemer, Cytoplasmic functions of the tumour suppressor p53, Nature 458 (2009) 1127–1130.
[55] F. Cottini, T. Hideshima, R. Suzuki, Y.T. Tai, G. Bianchini, P.G. Richardson, K.C. Anderson, G. Tonon, Synthetic lethal approaches exploiting DNA damage in aggressive myeloma, Cancer Discov. 5 (2015) 972–987.